CHEMISTRY
A EUROPEAN JOURNAL

DOI: 10.1002/chem.200501212

De Novo Design, Synthesis, and Characterization of Quinoproteins

Wen-Wu Li,*[a] Petra Hellwig,[b, c] Michaela Ritter,[b] and Wolfgang Haehnel*[a]

Abstract: Quinones and quinoproteins are essential redox components and enzymes in biological systems. Here, we report the de novo design, synthesis, and properties of model four-α-helix bundle quinoproteins. The proteins were designed and constructed from three different helices with 21 or 22 amino acid residues by chemoselective ligation to a cyclic decapeptide template. A free cysteine unit is placed at the hydrophobic core of the protein for binding of ubiquinone-0 and menaquinone-0 through a thioether bond. The quinoproteins with molecular weights of 11–12 kDa were characterized by electrospray ionization mass spectrometry, UV/Vis spectroscopy, size-exclusion chromatography, circular dichroism measurements, ^{1}H NMR spectroscopy, cyclic voltammetry, and redox-induced FTIR difference spectroscopy. The midpoint redox potentials at pH 8 in aqueous solution $E_{m,8}$ of thioether conjugates with *N*-acetyl cysteine methyl ester were 89 mV and −63 mV and with a synthetic protein 229 mV and 249 mV versus standard hydrogen electrode (SHE) for ubiquinone-0 and menaquinone-0, respectively. Detailed redox-induced FTIR difference spectroscopic studies of the model compounds and quinoproteins show the special resonance features for C=O bands at 1656–1660 and 1655–1665 cm^{-1} due to the sulfur substitution to ubiquinone-0 and menaquinone-0, respectively. The construction of model quinoproteins represents a significant step toward more complex artificial redox systems.

Keywords: cyclic voltammetry · IR spectroscopy · protein design · protein structures · quinones

Introduction

The de novo design and chemical synthesis of proteins play an important role in creating proteins with new functions.[1] The four-α-helix bundle as a simple and naturally occurring structural motif has become one of the most popular targets. Two main approaches have been utilized to construct such a scaffold. A self-assembly of amphiphilic helices was used by DeGrado et al.[2] and Dutton et al. to build a number of model proteins with biological redox cofactors including heme,[3a,b] iron sulfur clusters,[3c] metal ions like diiron,[3d] flavin,[3e] and Zn protoporphyrin IX,[3f] as well as radical-related side chains of Trp and Tyr.[3g] An approach proposed by Mutter is the covalent ligation of four helices to a peptide template termed template-assembled synthetic protein (TASP).[4] TASP has the potential advantage to reduce the folding problem with respect to the helix position and orientation. This allows the construction of antiparallel four-helix bundle proteins in a modular way from different helices. The advance of chemical synthesis and ligation techniques enables the construction of proteins.[5] As a result, models of hemoprotein, electron-transfer metalloproteins, and copper proteins have been constructed by our group.[6,7] Combinatorial synthesis and screening on a solid support has been shown to be an efficient way of selecting proteins with cofactors of desired properties.[7] The TASP or modular organized proteins (MOP) should also provide a suitable scaffold for an incorporation of a common redox cofactor-quinone to mimic its redox reaction in a protein environment.

[a] Dr. W.-W. Li, Prof. Dr. W. Haehnel
Institut für Biologie II/Biochemie
Albert-Ludwigs-Universität Freiburg
Schänzlestrasse 1, 79104 Freiburg (Germany)
Fax: (+49) 761-203-2601
E-mail: wenwu.li@biologie.uni-freiburg.de
haehnel@uni-freiburg.de

[b] Dr. P. Hellwig, M. Ritter
Institut für Biophysik
Johann Wolfgang Goethe-Universität Frankfurt
Max von Laue Strasse 1, 60438 Frankfurt/Main (Germany)

[c] Dr. P. Hellwig
Present address: Institut de chimie, UMR 7177-LC3 Laboratoire d'électrochimie, Université Louis Pasteur
4, rue Blaise Pascal, 67000 Strasbourg (France)

Supporting information (synthesis and characterization of benzyl- or *p*-methoxybenzyl-protected hydroquinoic acids, helical net representations of helix 1—3, and structures of some natural quinones) for this article is available on the WWW under http://www.chemeurj.org/ or from the authors.

Quinones including ubi-, mena-, and plastoquinone are essential components in membrane-bound electron-transfer reactions and conversion of redox energy to a H^+ ion gradient for ATP synthesis.[8] These are non-covalently bound quinones, as also found for pyrroloquinoline quinone.[9] However, there are a variety of covalently bound *o*-quinones[10] including topaquinone, lysine tyrosylquinone, tryptophan, and cysteine tryptophylquinone (CTQ)[11] in quinoenzymes for catalysis and electron transfer. CTQ is derived from an *o*-quinone-modified tryptophan side chain covalently crosslinked to a cysteine in amine dehydrogenase.[11] In addition, the noncovalently bound caldariella quinone (CQ)[12] in *Archaea* bacteria and 2-methylthio-1,4-menaquinone[13] in *Hydrogenobacter thermophilus* also possess a thioether bond. The thioether linkage is also quite common for other cofactors like heme (cytochrome *c*),[14] flavin (flavoproteins and blue-light receptors),[15] and open-chain tetrapyrroles (phycobiliproteins and phytochromes).[16]

The crystal structures of photosynthetic reaction centers, cytochrome bc_1 complexes and photosystem II[17] show complex interaction between quinones and their binding pockets including hydrogen bonds, electrostatic, and hydrophobic interactions. To mimic or design such a pocket for stable quinone binding is not yet possible by de novo design. However, it has been attempted to covalently bind quinone to proteins at a defined site in a similar way as in quinoenzymes. Thiol addition to quinones has enabled the site-specific binding of ubi-, mena-, or plastoquinone analogues to a free Cys residue of a de-novo-designed protein,[18a,b] an engineered cytochrome b_{562},[18c] and a natural protein like yeast iso-1 cytochrome *c*.[18d] The thioether bond linkage provides a basis for constructing novel proteins with quinones.

Redox-induced Fourier transform infrared (FTIR) difference spectroscopy is a very sensitive and useful tool to study the properties of quinones and their interaction with proteins.[19] The vibrational modes of ubiquinones in the natural biological systems like bacterial reaction centers,[20a,b] cytochrome bc_1,[20c] bo_3,[20d] and bd[20e] complexes from *E. coli* and CQ in the *aa*(3)-type quinol oxidase from *Aciidanus ambivalens*[20f] were identified by using this technique.

In this study, we report the design and synthesis of four-α-helix bundle proteins with 2,3-dimethoxy-5-methyl-1,4-benzoquinone (UQ-0) and 2-methyl-1,4-naphthoquinone (menadione, MQ-0) through thioether bond formation. The proteins and/or model thioether quinone adducts conjugated with *N*-acetyl cysteine derivatives were characterized by electrospray ionization (ESI) mass spectrometry, UV/Vis spectroscopy, circular dichroism (CD) measurements, size-exclusion chromatography, ^{1}H NMR spectroscopy, cyclic voltammetry, and redox-induced FTIR difference spectroscopy.

Results and Discussion

Protein design: The protein design concept is based on the TASP approach.[6] The molecular model of the four-helix bundle protein with UQ-0 is shown in Figure 1. It is designed to be an antiparallel four-helix bundle protein through assembly of three different amphipathic helices on a cyclic decapeptide template. The two helices H2 of the same kind are oriented antiparallel to the other two helices H1 and H3. Their amino acid sequences (helical net representation in the Supporting Information) are:

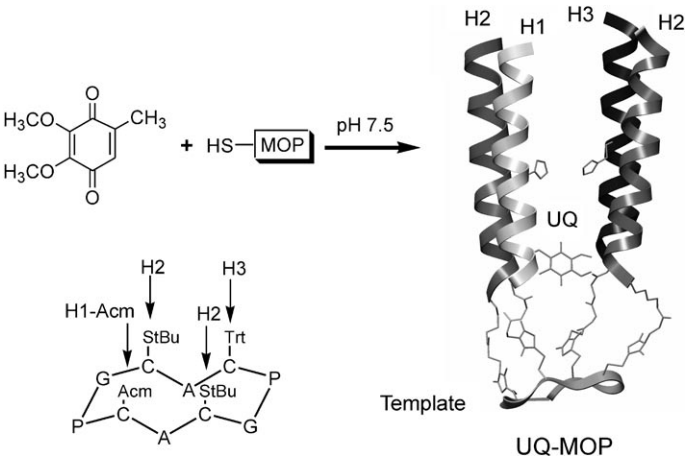

Figure 1. Structural model of the de-novo-designed four-α-helix bundle quinoprotein UQ-MOP. UQ-0 was coupled to the Cys unit of the apoprotein through thioether bond formation. The backbone of the cyclic decapeptide template and the helices are shown as ribbon. Amino acid side chains are shown to illustrate the thioether linkage of the four Cys units of the template with the succinimidopropionyl (Sp) moiety formed by addition of SH to the Mp group at the N-terminal Gly of H1 and H3 and the C-terminal Lys of H2. The UQ-0 group is shown as sticks. The program INSIGHT II (Accelrys Inc. San Diego, CA) was used.

H1-Acm: Mp-GNA**C**(Acm)EELRKKHQELAEKLQKW-$CONH_2$

H2: Ac-NLEQFEKALKQGEELAKKLAK(Mp)-$CONH_2$

H3: Mp-GNALEELAKKHQQLAEALQKL-$CONH_2$

Acm = acetamidomethyl, Mp = 3-maleimidopropionyl.

The sequence of amino acids and the design principles are similar to those previously described[6] except for Cys4 (highlighted in bold in the sequence above) of H1 that is positioned in the hydrophobic face and protected by the Acm unit for quinone binding after selective deprotection. His11 of helices H1 and H3 also at the hydrophobic face have been introduced as ligands for later binding of other cofactors like heme or photoactive Zn protoporphyrin IX.[3f,6d]

Synthesis of quinoproteins and model compounds: The four-helix bundle protein with a free Cys residue was synthesized as published.[6a,b] The cyclic decapeptide template with four Cys residues protected by three orthogonal groups (trityl (Trt), *tert*-butylthio (S*t*Bu), and Acm)[21] in Figure 1 (left) and three different helices were synthesized by Fmoc solid-

phase peptide synthesis (SPPS). Helices H1 and H3 and helix H2 were modified at the N-terminal amino groups and the ε-amino group of the C-terminal Lys unit, respectively, by 3-maleimidopropionic acid and ligated to the template as described previously.[6a,b] Final deprotection of the Acm group of H1 in the four-helix bundle yielded a modular organized protein termed MOP with one free thiol group. UQ-0 (Figure 1) and MQ-0 in excess were chemoselectively coupled to the free Cys residue of MOP to form UQ-MOP and MQ-MOP, respectively. The ESI mass spectra of MOP and UQ-MOP (Figure 2) show the correct masses with the

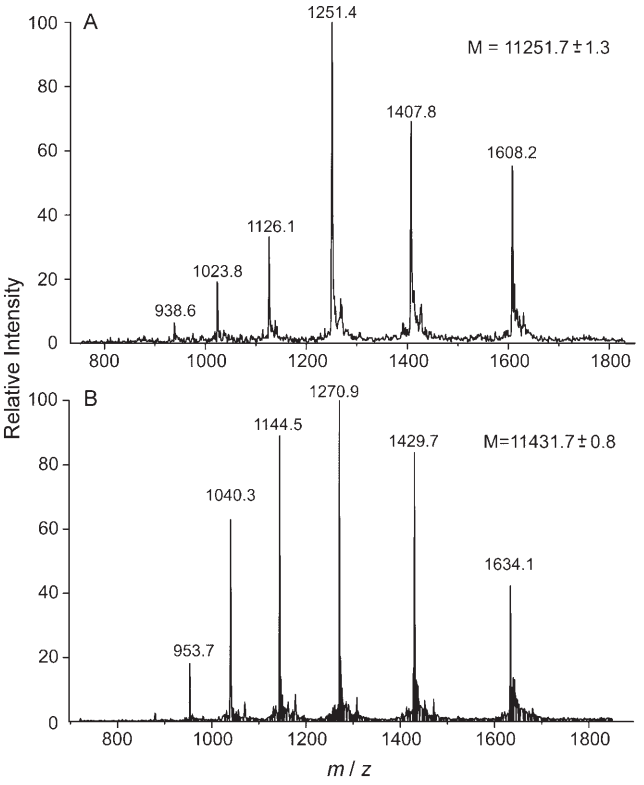

Figure 2. Electrospray ionization mass spectra of purified MOP (A) and UQ-MOP (B).

difference of mass 180 corresponding to only one molecule of UQ-0. The masses determined during the synthesis were compared with the calculated values in Table 1. They indicate the correct construction of the four-helix bundle protein as well as binding of UQ-0 and MQ-0 to the free Cys unit of MOP.

Model thioether quinone adducts were prepared through coupling UQ-0 and MQ-0 with different Cys derivatives. The amino group of Cys should be blocked (by acetylation) to avoid cyclization through formation of a Schiff base with one carbonyl group of the quinone.[22] The conjugate of *N*-acetyl cysteine amide with UQ-0 was found to be unstable owing to a similar Schiff base formation with the even less electronegative amide group (data not shown). Therefore, *N*-acetyl cysteine ((*N*-Ac)Cys) and *N*-acetyl cysteine methyl

Table 1. Masses of the intermediates during the synthesis and assembly of the proteins.

Peptides and proteins	Calcd average mass [Da]	Found mass [Da]
T(S*t*Bu)$_2$(Trt)(Acm)	1353.0	1352.5
T(Trt)(Acm)	1176.6	1176.6
H2	2608.0	2607.2 ± 0.1
H3	2482.8	2482.7 ± 0.4
H1(Acm)	2760.1	2760.0 ± 0.1
T(Sp-H2)$_2$ (Trt)(Acm)	6392.5	6392.8 ± 0.9
T(Sp-H2)$_2$ (Acm)	6151.3	6150.2 ± 0.3
T(Sp-H2)$_2$ (Sp-H3)(Acm)	8634.1	8632.8 ± 0.4
T(Sp-H2)$_2$ (Sp-H3)	8562.9	8562.5 ± 0.6
T(Sp-H2)$_2$ (Sp-H3)[Sp-H1-(Acm)]	11323.0	11324.6 ± 0.7
MOP	11251.8	11251.7 ± 1.3
UQ-MOP	11432.0	11431.7 ± 0.8
MQ-MOP	11422.0	11421.2 ± 1.9

ester ((*N*-Ac)CysOMe) were coupled to UQ-0 and MQ-0. In all coupling reactions, the oxidized thioether quinone adducts together with their reduced forms, parent quinones, and their reduced forms were observed by reverse-phase high-performance liquid chromatography (HPLC) and ESI-MS.

To realize quinone binding to peptides or proteins, we initially tried to incorporate hydroquinonoic acids (2,5-dihydroxyphenylacetic acid and 1,4-dihydroxynaphthalene-2-carboxylic acid) into a peptide through amide bond formation in SPPS. The purpose was to synthesize a quinone-containing peptide as a building block from different quinones that can be incorporated into synthetic proteins. Therefore, the acid-sensitive protecting groups such as benzyl (Bn)- or *p*-methoxybenzyl (PMB)[23]-protected hydroquinonoic acids were prepared through the following steps: 1. Selective protection of the carboxy group by methyl or ethyl ester; 2. Protection of the phenol groups by Bn or PMB units; 3. Selective alkaline hydrolysis of ester (synthesis details available in the Supporting Information). The protected hydroquinonoic acids were used for coupling to the ε-amino group of Lys4 instead of Cys(Acm) in helix 1 (H1) after selective cleavage of the allyloxycarbonyl group[24] in SPPS. However, we found with ESI-MS that the products generated from the coupling, deprotection, and/or cleavage by trifluoroacetic acid were complex and did not include the desired component. It seemed not to be possible with this method to incorporate the hydroquinones into a peptide.

Therefore, a specific modification of a Cys residue in a protein by quinones was attempted. Halogen-methyl-substituted quinones like 3-bromomethyl-2-methyl-1,4-naphthoquinone[25] and 3-chloromethyl-2-methyl-1,4-naphthoquinone were synthesized (see Supporting Information) that are known as bioreductive activation agents for the treatment of cancer cells.[26] They showed strong reactivity toward not only the Cys but also other amino acids (data not shown). However, the selective thiol addition to UQ-0 and MQ-0 as described above allowed the successful construction of model quinoproteins. In addition to MQ-0, 2-

methyl-3-bromo-1,4-naphthoquinone[27] synthesized from MQ-0 could bind more efficiently to a Cys residue of the protein through thiol addition and bromide elimination with a higher yield of about 60%. Following a similar reaction, 3-methyl-indole-6,7-dione[28] and 6-methyl-4,7-thionaphthene-quinone[29] are suggested to specifically bind to a Cys residue to generate CTQ and CQ mimetics, respectively.

Characterization of quinoproteins and model thioether quinones

UV/Vis spectroscopy: Figure 3A shows the UV/Vis spectra of UQ-0, UQ-MOP, and UQ-(*N*-Ac)Cys in aqueous buffer, pH 8.0. The intense π–π* transition bands are at 267 nm for

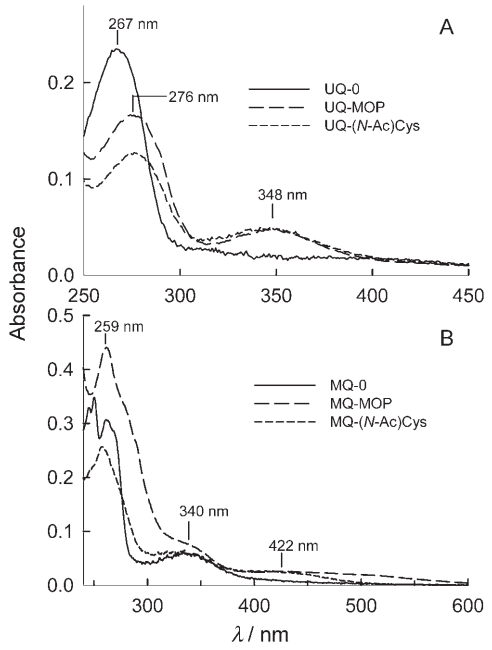

Figure 3. UV/Vis spectra of UQ-0, UQ-(*N*-Ac)Cys, UQ-MOP (A); MQ-0, MQ-(*N*-Ac)Cys, MQ-MOP (B). The concentrations of quinones and quinoproteins are at 30 μM in 50 mM Tris-HCl, pH 8.0, and 100 mM NaCl. Main peaks of quinones are labeled except those of MQ-0 showing major π–π* transition bands at 246, 249, and 262 nm, and a broad low-intensity band at 334 nm also found with MQ-(*N*-Ac)Cys.

UQ-0 and 276 and 348 nm for UQ-(*N*-Ac)Cys and UQ-MOP. A more intense absorption at about 276 nm for UQ-MOP than for UQ-(*N*-Ac)Cys is ascribed to Trp in helix H1. This indicates that sulfur substitution to UQ-0 causes a red shift from 267 to 276 nm as well as a new medium band at 348 nm. Figure 3B shows the UV/Vis spectra of MQ-0, MQ-MOP, and MQ-(*N*-Ac)Cys. The absorptions around 250 nm for the fine structure of MQ-0 are replaced by a single major peak at 259 nm for MQ-(*N*-Ac)Cys and MQ-MOP. The sulfur substitution causes also a new band to arise in the spectrum at 422 nm. In addition, there is a more intense absorption for MQ-MOP than for MQ-(*N*-Ac)Cys not only in the region of aromatic amino acids, but also in the visible range from 450 to 600 nm. This may indicate an interaction of MQ-0 with the protein. The absorption spectra of MQ-0 and MQ-(*N*-Ac)Cys in buffer are similar to those previously measured in methanol.[30] To summarize, sulfur substitution into quinones significantly changes their absorption spectroscopic properties.

Size-exclusion chromatography: Figure 4 shows size-exclusion chromatograms of the modular proteins and the cali-

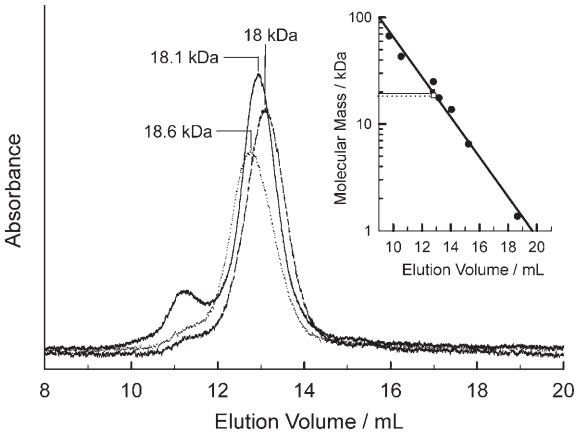

Figure 4. Size-exclusion chromatography of the synthetic proteins. The size-exclusion chromatograms of MOP (•••••), UQ-MOP (-----), and MQ-MOP (——) were recorded at a flow rate of 0.5 mL min^{-1} with a Pharmacia Superdex 75 (1×30 cm) size-exclusion FPLC column equilibrated with 50 mM potassium phosphate buffer (pH 7) and 100 mM NaCl. Retention volumes of the proteins were determined by following the absorbance at 215 nm. The inset shows the elution volumes of a set of globular proteins (●) (low molecular weight kit). The straight line is the linear regression of the calibration values. The elution volumes of MOP (■) and UQ-MOP (□) at a concentration of 80 μM indicate molecular masses of 18.6 and 18 kDa, respectively.

bration with a set of globular proteins with a Sephadex 75 column. The elution times and symmetrical peaks of MOP, UQ-MOP, and MQ-MOP indicate apparent molecular masses in the range of 18 kDa, consistent with monomers. The elution of a minor peak at 38 kDa indicates that 20% of total MQ-MOP forms a dimer. The small fraction of dimer found with MQ-MOP may be attributed to the larger size of MQ-0 as compared to UQ-0 being not fully adapted to the space between the four helices. The globular form of monomeric UQ-MOP seems to be slightly smaller than that of MOP, consistent with a compact structure of UQ-MOP.

Secondary structures of quinoproteins: Circular dichroism spectra of MOP, UQ-MOP, and MQ-MOP in Figure 5 show characteristic minima at 222 and 208 nm with a ratio $[\theta_{222}]/[\theta_{208}]=0.87$, indicating an α-helical secondary structure. The mean residue molar ellipticities at 222 nm θ_{222} were −19000, −15000, −15000 deg cm^2 dmol^{-1} for MOP, UQ-MOP, and MQ-MOP, respectively. These values are based on the extinction coefficient of tryptophan at 280 nm for MOP and those of quinone in the thioethers of cysteine

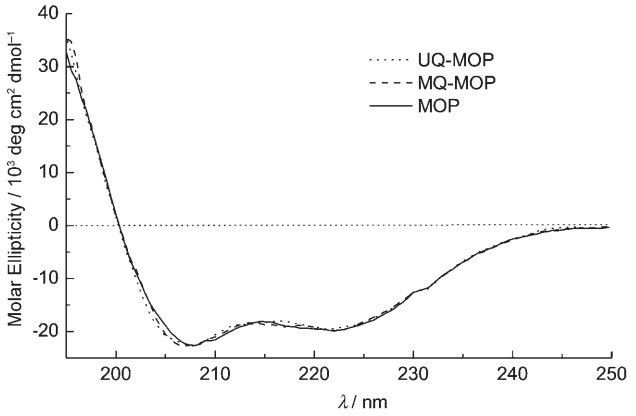

Figure 5. Circular dichroism spectra of MOP (12 μM) (——), UQ-MOP (17 μM) (•••••), and MQ-MOP (22 μM) (-----) in 20 mM potassium phosphate, pH 7 at 20 °C. For details see text.

at 348 and 340 nm for UQ-MOP and MQ-MOP, respectively. The effect of the protein is not known. Therefore, the CD spectra have been normalized to facilitate a direct comparison. They are almost identical except for a minor shift of the UQ-MOP and MQ-MOP spectrum towards short wavelengths indicating a slightly increased fraction of random coil conformation as compared to MOP. The values of the ellipticity suggest a helicity in the range of 50–65 % if 100 % helicity is referred to a value of −35 700[31] or −32 200 deg cm^2 dmol^{-1} as determined from tropothyosin.[32] According to the model in Figure 1 a helicity of 89 % is expected. CD spectra and gel filtration experiments do not indicate substantial changes of packing and helicity of the four-helix bundle by insertion of the quinones.

Figure 6 shows ^{1}H NMR spectra of MOP (A) and UQ-MOP (B) in the aromatic range. The resonances show a

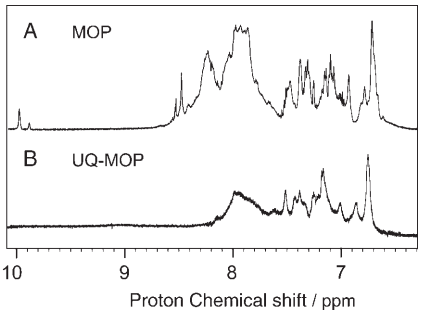

Figure 6. One-dimensional ^{1}H NMR spectra in the aromatic and amide proton region of the proteins MOP (A) and UQ-MOP (B). Experimental conditions are given in the Experimental Section. Chemical shifts are given in ppm from DSS.

good dispersion of chemical shifts for MOP with a resolution similar to those of other designed four-helix bundle proteins.[3b,7b] The ^{1}H NMR signals of UQ-MOP show a significant line broadening. This could be caused by an effect of the quinone on the packing of the hydrophobic core in the four-helix bundle or an association at the high concentration used for the NMR experiment that is not observed at the low concentration used for the experiments that produced the data presented in Figure 4. The packing of the helices with quinones located in the hydrophobic core of the protein is currently under investigation and will be optimized by a computational and combinatorial[7] approach.

Electrochemistry: The midpoint redox potentials of model thioether quinone adducts and quinoproteins were characterized by cyclic voltammetry in aqueous buffer. Cyclic voltammograms (CV) show the half-wave reduction potentials of UQ-(*N*-Ac)CysOMe (Figure 7 A) and MQ-(*N*-Ac)Cys-

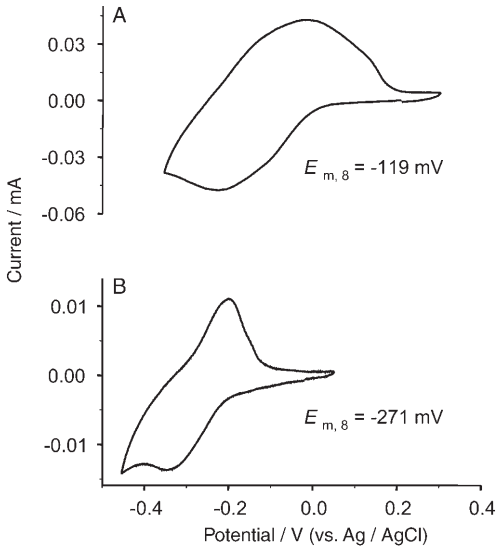

Figure 7. Cyclic voltammograms of UQ-(*N*-Ac)CysOMe (A) and MQ-(*N*-Ac)CysOMe (B) in aqueous buffer, pH 8.0, versus the Ag/AgCl reference electrode.

OMe (Figure 7 B) as $E_{m,8}=89$ mV and $E_{m,8}=-63$ mV, respectively, versus SHE (208 mV Ag/AgCl reference electrode) in aqueous buffer, pH 8.0. Compared to their respective redox potentials of unmodified UQ-0 ($E_{m,8}=102$ mV,[33] or $E_{m,7}=180$ mV[18c]) and MQ-0 ($E_{m,8}=-61$ mV)[33b,34,35] sulfur substitution to the quinones does not significantly change their midpoint redox potentials in aqueous solution. This is consistent with the redox potentials observed in acetonitrile.[18d] A variation of side chains by (*N*-Ac)Cys[35] and glutathione[35,36] introduced to MQ-0 could have a minor effect on the redox potentials. A small change of the one-electron reduction potential value by glutathionyl substitution to MQ-0 has been found by using pulse radiolysis.[37] In contrast to the methyl esters the CV of UQ-(*N*-Ac)Cys and MQ-(*N*-Ac)Cys showed complex phenomena in aqueous solution (not shown) and also in acetonitrile, attributable to the influence of the carboxy group in the side chain.[18d]

Figure 8 shows the half-wave reduction potentials of UQ-MOP(L) (Figure 8 A) and MQ-MOP(L) (Figure 8 B) as $E_{m,8}$ 229 and 249 mV, versus SHE (208 mV Ag/AgCl reference electrode) in aqueous buffer, pH 8.0, respectively. In these

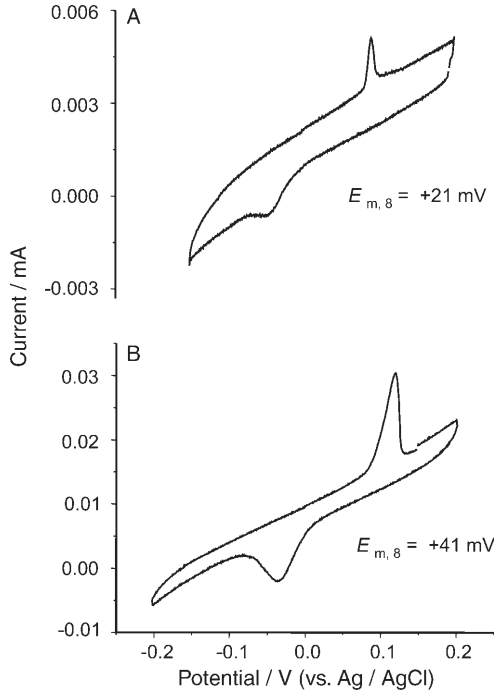

Figure 8. Cyclic voltammograms of UQ-MOP(L) (A) and MQ-MOP(L) (B) in aqueous buffer, pH 8.0.

proteins His11 of helix H3 was replaced by a Leu residue. The midpoint redox potential of the quinones in the protein is significantly shifted by +140 and +312 mV relative to those of UQ-(*N*-Ac)CysOMe and MQ-(*N*-Ac)CysOMe, respectively. In particular, the large shift of the MQ potential was unexpected. The positive redox potentials indicate that the amino acid residues of the four-helix bundle protein have a strong effect on the quinones. A nearby Arg residue may contribute to this effect. The influence of the protein environment in an engineered cytochrome b_{562} on the redox potential of UQ-0 has been found to be minimal (about +25 mV).[18c] The modulation of the redox potential of quinones by protein interactions in photosynthetic reaction centers has been analyzed in detail.[38]

Redox-induced FTIR difference spectroscopy: Figure 9 A shows the direct comparison of the oxidized-minus-reduced FTIR difference spectra of free UQ-2, UQ-(*N*-Ac)Cys, and UQ-(*N*-Ac)CysOMe for a potential step from −0.5 to 0.5 V. The positive signals correlate with the oxidized form and the negative modes with the reduced form of the sample. In the electrochemically induced FTIR difference spectrum of UQ-2 in aqueous solution (Figure 9 A, top), the split ν(C=O) modes of the oxidized quinone are at 1664 and 1648 cm^{-1} and the ν(C=C) mode is at 1610 cm^{-1}.[39a,20b] At 1288 and 1264 cm^{-1} the signals from the C−OCH_3 vibrations of the 2- and 3-methoxy groups contribute.[39b] The ring modes of the fully reduced and protonated forms of ubiquinol contribute to the signals at 1494, 1470, 1430, and 1386 cm^{-1}. In the spectra (Figure 9 A, middle and bottom) of the two (*N*-Ac)Cys and (*N*-Ac)CysOMe bound UQ-0,

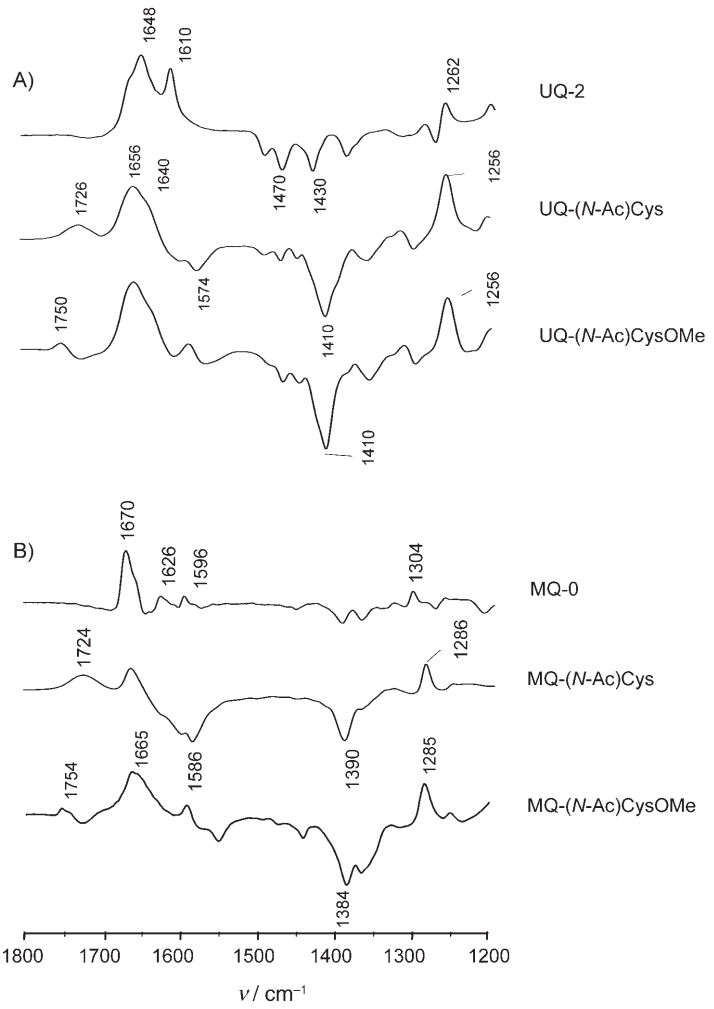

Figure 9. Oxidized-minus-reduced FTIR difference spectra of free UQ-2, UQ-(*N*-Ac)Cys, and UQ-(*N*-Ac)CysOMe (A); free MQ-0, MQ-(*N*-Ac)Cys, and MQ-(*N*-Ac)CysOMe (B) for a potential step from −0.5 to 0.5 V. For details see Experimental Section.

UQ-(*N*-Ac)Cys and UQ-(*N*-Ac)CysOMe shifts of the vibrational modes can be expected due to the changed symmetry of the ring by sulfur substitution. Since all modes in the quinone are coupled, a variation on one side of the ring, will affect all observed vibrations, as shown before by site-specific labeling.[20d,39a,b]

The ν(C=O) mode of both C=O groups can be tentatively attributed to be involved in the broad signals at 1656 and 1640 cm^{-1} in both spectra. A further signal, that involves coordinates from the quinone, is seen at 1256 cm^{-1} and is attributed to the C−OCH_3 vibrations of the 2- and 3-methoxy groups. The position of the ν(C=C) mode, however, is not clear. This spectral feature seems to be overlapped by a strong negative feature at 1574 cm^{-1} or shifted up towards the very broad signal at 1656–1640 cm^{-1}. The signals at 1726 and 1750 cm^{-1} for UQ-(*N*-Ac)Cys and UQ-(*N*-Ac)CysOMe, respectively, arise at a position typical for a ν(C=O) mode, these signals might be attributed to the introduced side chain. Whereas for the UQ-(*N*-Ac)Cys variant a protonation

reaction could be inferred, the signal at 1574 cm^{-1} might involve contributions from side-chain variations. Another strong feature arising in the variants is a strong negative mode at 1410 cm^{-1}. Though this signal is located in a spectral region including several vibrations, like ring modes and the O–H vibrational mode, an assignment to the $\delta(S-CH_2)$ vibration of the introduced side chain seems possible.

Figure 9B presents the direct comparison of the oxidized-minus-reduced FTIR difference spectra of free MQ-0, MQ-(*N*-Ac)Cys, and MQ-(*N*-Ac)CysOMe for a potential step from −0.5 to 0.5 V. In the FTIR redox difference spectrum of MQ-0, the split ν(C=O) mode is at 1670 cm^{-1} with a shoulder at 1658 cm^{-1}. The ν(C=C) mode of the quinoid ring is at 1626 cm^{-1} and of the aromatic ring is at 1596 cm^{-1}. The mode at 1304 cm^{-1} has been previously attributed to a coupled C–C/C=C vibration.[39b] The ring modes of the fully reduced and protonated form could contribute to the signals at 1394 and 1368 cm^{-1}, however, they have not been fully understood yet. Also for the MQ-(*N*-Ac)Cys and MQ-(*N*-Ac)CysOMe, the binding of the side chain induces several shifts of the different quinone modes (Figure 9B, middle and bottom). The ν(C=O) mode is downshifted to 1665 cm^{-1} and the ν(C=C) mode, though overlaid by the strong negative mode at 1586 cm^{-1}, can still be noted at 1620 cm^{-1} for the quinoid ring and at 1594 cm^{-1} of the aromatic ring. At 1286 and 1285 cm^{-1} the downshifted signal of the coupled C–C/C=C vibration is visible. In line with our observations of the UQ-(*N*-Ac)CysOMe (Figure 9A), bands at typical positions for a ν(C=O) mode can be seen coupled with the oxidized form at 1724 and at 1754 cm^{-1} with the reduced form at 1586 and 1390 cm^{-1}.

Figure 10 shows the oxidized-minus-reduced FTIR difference spectra of UQ-MOP (A) and MQ-MOP (B) for a potential step from −0.5 to 0.5 V. The spectra show the vibrational modes of the bound quinones significantly shifted due to the binding to the peptides. In the case of the UQ-MOP the ν(C=O) mode could give rise to the band at 1660 cm^{-1}

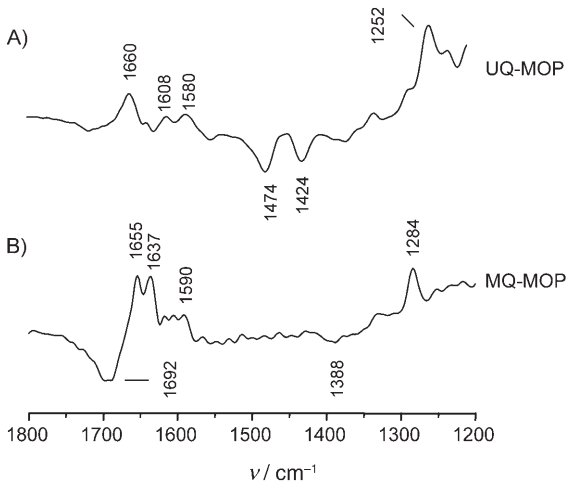

Figure 10. Oxidized-minus-reduced FTIR difference spectra of UQ-MOP (A) and MQ-MOP (B) for a potential step from −0.5 to 0.5 V. For details see Experimental Section.

and the ν(C=C) mode in the shoulder at approximately 1608 cm^{-1}. The positive signal seen at 1256 cm^{-1} is attributed to the C–OCH_3 vibrations of the 2- and 3-methoxy groups, however, it may also involve vibrations of the C–S linkage. The ring modes of the fully reduced and protonated forms of ubiquinol are tentatively assigned to the signals at 1474, 1424, and 1356 cm^{-1}. Also here vibrations from the thioether linkage may be expected.

In addition to the quinone signals, ν(C=O) (amide I) and the coupled ν(CN/NH) (amide II) backbone vibrations could be involved in the spectra observed here, that is, between 1690 and 1600 cm^{-1} (amide I) and between 1580 and 1520 cm^{-1} (amide II). Signals that are typical of the α-helical secondary structure elements are likely to contribute to the broadened signal at 1560 cm^{-1}. Comparing the data for the quinone bound by (*N*-Ac)Cys and MOP, similar shifts of the vibrational modes of about 5–10 cm^{-1} are seen, each shifted in the same direction, confirming that these effects could arise from the change in symmetry of the ring, affecting all coupled modes.

For MQ-MOP, the ν(C=O) and ν(C=C) vibrations contribute to a large differential feature between 1690 and 1630 cm^{-1}, probably partially overlapped by vibrations due to the amide I. Clear assignments are not possible without labeling of the C=O groups. Overall the difference spectra for MQ-MOP and UQ-MOP in Figure 9 are quite different, indicating that the quinone modes dominate the spectra. For MQ-MOP (Figure 9B) the ν(C=O) signal is shifted down to 1654 cm^{-1} and the ν(C=C) signals can be seen between 1600 and 1590 cm^{-1}. At 1284 cm^{-1} the downshifted signal of the coupled C–C/C=C vibration is visible. Possible contributions of the signals due to the ν(C=O) (amide I) backbone vibrations are seen between 1690 and 1600 cm^{-1}. No noteworthy signals in the spectral region for the coupled ν(CN/NH) (amide II) vibrations can be seen. Comparing the data for the quinone bound by (*N*-Ac)Cys and MOP, similar shifts of the vibrational modes of about 5–10 cm^{-1} are seen, each shifted in the same direction, confirming that these effects could arise from the change in symmetry of the ring, affecting all coupled modes.

Significant changes of bands due to C=O were found in the redox-induced difference FTIR spectra for both adducts of quinones with Cys derivatives and protein. In addition, the proton effect resulting from carboxylic acid was observed at 1726 cm^{-1} for (*N*-Ac)Cys conjugates that was confirmed by the study of their (*N*-Ac)CysOMe conjugates. Previous FTIR studies on the CQ[20d] showed quite different spectral features from those of our model thioether quinone adducts due to the different ring system despite having a similar thioether bond. The FTIR and electrochemical studies of thioether-bound quinone adducts should also contribute to the understanding of their physicochemical properties as well as the toxicological activity of quinones and thioether quinone adducts.[33a,37]

Conclusion

Model quinoproteins were de novo designed and constructed for the first time on the basis of the TASP strategy. Different methods of ligation of quinones to peptides or protein were tried. Finally the thioether ligation was successful by a direct thiol addition to trisubstituted quinones including UQ-0 and MQ-0. The proteins with 96 amino acid residues (M_W: 11–12 kDa) were chemically synthesized under the control of each step by ESIMS. Their structural properties and the effect of quinone binding were characterized by gel filtration, CD measurements, and ^{1}H NMR spectroscopy. They all showed the α-helical structure as designed. The absorption and electrochemical properties of model thioether quinone adducts were characterized by UV/Vis spectroscopy, cyclic voltammetry, and redox-induced FTIR difference spectroscopy. The protein appeared to have a substantial effect on the midpoint redox potential in contrast to the thioether ligation. The FTIR difference spectra disclosed special resonance features for thioether quinone adducts. The further insertion of a flavin and heme cofactor into these complexes may facilitate the studies of light-induced electron transfer in designed redox proteins.[3e,6b,40] Therefore, the construction of model quinoproteins represents a basic and significant step toward artificial photoenzymes and more complex redox systems.

Experimental Section

General: UQ-0, MQ-0, *N*-acetyl cysteine [(*N*-Ac)Cys], *N*-acetyl cysteine methylester [(*N*-Ac)CysOMe], and all other chemicals of the highest available grade were obtained from Aldrich/Sigma, *N*,*N*′-diisopropylethylamine (DIEA), *o*-(benzotriazol-1-yl)-1,1,3,3,-tetramethyluronium tetrafluoroborate (TBTU), 5-(4-(aminomethyl)-3,5-bis(methyloxy)phenoxy)valeric acid/poly(ethylene glycol)/polystyrene (PAL-PEG-PS) resin, and 9-fluorenylmethyloxycarbonyl (Fmoc) protected amino acids were purchased from Perspective Biosystems (Framingham, MA), and preloaded Fmoc-Gly-NovaSyn TGT resin was from Nova Biochem. ^{1}H NMR data of the model quinones were recorded on a Bruker 250 or 400 MHz spectrometer. [D$_6$]DMSO, CH_3COCD_3, or $CDCl_3$ were used as solvents.

Electron-impact (EI) mass spectrometry data were recorded by a Finnigan MAT 445 apparatus (EI, 70 eV). ESI mass spectra were recorded by a Finnigan TSQ 700 tandem quadrupole mass spectrometer with an electrospray interface. Peptides were dissolved in 10 μL of 50% CH_3CN with 0.1% TFA for ESI-MS.

Reverse-phase HPLC: Analytical HPLC was carried out on a Waters model 600E system equipped with a Waters model 996 photodiode array detector. A YMC-Pack ODS-AQ stainless-steel column (150×4.6 mm, 5 μm) was run at a flow rate of 1 mL min^{-1}. Preparative HPLC was performed on a Waters DeltaPak C18 PrePak column (300×40 mm, 15 μm) at a flow rate of 50 mL min^{-1}. Half-preparative HPLC was performed on a YMC-Pack ODS column (250×20 mm, 15 μm) at a flow rate of 10 mL min^{-1}. The runs used different gradients of 0.1% TFA (buffer A) versus 4:1 acetonitrile/water plus 0.1% TFA (buffer B).

Synthesis of four-helix bundle quinoproteins: The four-helix bundle protein was assembled by consecutive deprotection of three different Cys protecting groups (Acm, S*t*Bu, and Trt) of cyclic decapeptide template (T), T(S*t*Bu)$_2$(Trt)(Acm), cyclo[C(Acm)-A-C(S*t*Bu)-P-G-C(Trt)-A-C-(S*t*Bu)-P-G-].[6a,b] Each deprotection was followed by chemoselective coupling of one of the three unprotected 3-maleimidpropionyl (Mp) helical peptides to the template in solution as described.[6] UQ-0 was chemoselectively coupled to the MOP by adding UQ-0 (3.6 mg, 20 μmol) in acetonitrile (0.2 mL) to a solution of MOP (11.4 mg, 1 μmol) in previously degassed Tris buffer (5.0 mL, 50 mM), pH 7.5 with 6 M GuHCl/acetonitrile (3:2) and was stirred for 6 h under argon and in the dark at room temperature. A minimum of $K_3[Fe(CN)_6]$ was added and stirred for 10 min. The ubiquinone-modified protein was purified by reversed-phase HPLC and lyophilized to give 4.5 mg of UQ-MOP (yield 38%). The coupling of MQ-0 (1.0 mg, 5.8 μmol) to MOP (3.0 mg, 0.27 μmol) was performed in the same manner as UQ-MOP to yield 1.5 mg of MQ-MOP (yield 49%).

***N*-Acetyl-S-(2,3-dimethoxy-5-methyl-1,4-benzylquinonyl-6)cysteine, UQ-(*N*-Ac)Cys**: (*N*-Ac)Cys (81.5 mg, 0.5 mmol) was added to a solution of UQ-0 (182 mg, 1.0 mmol) in ethanol (4 mL) and water (1 mL). The solution was stirred overnight. The mixture was diluted with water (20 mL), extracted with ethyl acetate (2×20 mL), and the solvent was evaporated. Preparative HPLC was used for purification and yielded UQ-(*N*-Ac)Cys as a red solid (50 mg, yield 29%). ^{1}H NMR (250 MHz, [D$_6$]acetone, 25 °C): δ = 7.40 (d, 1H; NH), 4.60 (m, 1H; CH), 3.88 (s, 6H; 2×OCH_3), 3.52 (dd, 1H; CH), 3.28 (dd, 1H; CH), 2.05 (s, 3H; CH_3), 1.82 ppm (s, 3H; CH_3); ^{1}H NMR (500 MHz, 90% 20 mM Tris-HCl, pH 7.5, 10% [D$_2$]water): δ = 8.10 (d, 1H; NH), 4.31 (m, 1H; CH), 3.88 (s, 6H; 2×OCH_3), 3.47 (dd, 1H; CH), 3.19 (dd, 1H; CH), 2.06 (s, 3H; CH_3), 1.89 ppm (s, 3H; CH_3); MS (ESI): *m*/*z*: 344 [*M*+H$^+$], 366 [*M*+Na$^+$], 709 [2*M*+Na$^+$]; MS (EI, 70 eV): *m*/*z* (%): 343 (4), 284 (7), 227 (76), 216 (100), 214 (44), 201 (20), 199 (12), 183 (15), 181 (11).

***N*-acetyl-S-(2,3-dimethoxy-5-methyl-1,4-benzylquinonyl-6)cysteine methyl ester, UQ-(*N*-Ac)CysOMe**: (*N*-Ac)CysOMe (35 mg, 0.2 mmol) was added to a solution of UQ-0 (75 mg, 0.41 mmol) in ethanol (2 mL) and water (1 mL). The solution was stirred overnight. Preparative HPLC was used for purification and yielded UQ-(*N*-Ac)CysOMe as a red solid (8 mg; yield 11%). ^{1}H NMR (250 MHz, [D$_6$]DMSO, 25 °C): δ = 6.38 (d, 1H; NH), 4.78 (m, 1H; CH), 4.00 (s, 6H; 2×OCH_3), 3.70 (s, 3H; CH_3), 3.48 (m, 2H; CH), 2.18 (s, 3H; CH_3), 1.98 ppm (s, 3H; CH_3); MS (ESI): *m*/*z*: 358 [*M*+H$^+$], 380 [*M*+Na$^+$].

***N*-acetyl-S-(2-methly-1,4-naphthoquinonyl-3)cysteine methylester, MQ-(*N*-Ac)CysOMe**: (*N*-Ac)CysOMe (90 mg, 0.51 mmol) was added to a solution of MQ-0 (182 mg, 1.06 mmol) in ethanol (6 mL). The solution was stirred overnight. The product was purified by preparative HPLC to give MQ-(*N*-Ac)CysOMe (58 mg; yield 33%). ^{1}H NMR (250 MHz, [D$_6$]DMSO, 25 °C): δ = 8.35 (d, 1H; NH), 7.95 (m, 2H; CH-5, CH-8), 7.68 (m, 2H; CH-6, CH-7), 4.48 (m, 1H; CH), 3.50 (s, 3H; CH_3), 3.40 (m, 2H; CH), 2.21 (s, 3H; CH_3), 1.67 ppm (s, 3H; CH_3); MS (ESI): *m*/*z*: 348 [*M*+H$^+$], 370 [*M*+Na$^+$].

UV/Vis spectroscopy: UV/Vis spectra of all the compounds were recorded on a Shimadzu spectrophotometer. All concentrations of model quinones and quinoproteins were 30 μM in 50 mM Tris-HCl buffer, pH 8.0, and 100 mM NaCl. The spectra were acquired at room temperature.

Circular dichroism spectroscopy: CD spectra were recorded on a Jasco 700 spectrometer. A quartz cuvette with a path length of 1 mm was used. The concentrations of MOP, UQ-MOP, and MQ-MOP in 20 mM potassium phosphate buffer (pH 7.0) were determined to be approximately 12, 17, and 22 μM through the absorbance of the tryptophan residue at 280 nm (ε = 5700 cm^{-1} M^{-1}), thioether ubiquinone adduct at 348 nm (ε = 3000 cm^{-1} M^{-1}, determined from UQ-(*N*-Ac)Cys), and thioether menaquinone adduct at 340 nm (ε = 5000 cm^{-1} M^{-1}) for MOP, UQ-MOP, and MQ-MOP, respectively.

Size-exclusion chromatography: Size-exclusion chromatography was performed on a Hewlett–Packard model 1050 Ti HPLC system equipped with a Pharmacia Superdex 75 column (10×300 mm) equilibrated with 50 mM potassium phosphate buffer (pH 7) and 100 mM NaCl. To estimate the molecular mass of apoprotein and quinoproteins, the column was calibrated with bovine serum albumin (67 kDa), ovalbumin (43 kDa), α-chymotrypsinogen (25 kDa), myoglobin (17.6 kDa), ribonuclease A (13.7 kDa), aprotinin (6.5 kDa), and vitamin B_{12} (1.36 kDa). Peptide and protein samples were eluted at a flow rate of 0.5 mL min^{-1}, the absorbance was monitored at 215 nm.

^{1}H NMR spectroscopy: ^{1}H NMR data were recorded on a Bruker 500 MHz spectrometer. Spectra were acquired with MOP and UQ-MOP

at a concentration of 1.3 mM and 0.7 mM, respectively, in 20 mM Tris/HCl, pH 7.5 and 10% D_2O at 301 K.

Cyclic voltammetry: Cyclic voltammetry of quinones in aqueous buffer solution was carried out in an electrochemical set up consisting of a gold mesh as working electrode, a platinum counter electrode, and a 3 M KCl/Ag/AgCl reference electrode, in an ultrathin cell as reported before.[41]

Fourier transform infrared difference spectrometry: For electrochemistry, samples were dissolved in 100 mM phosphate buffer containing 100 mM KCl at a concentration typically in the range of 1 mM. The ultra-thin-layer spectroelectrochemical cell for the UV/Vis and IR measurements was used as previously described.[39] Sufficient transmission in the 1800–1000 cm^{-1} range, even in the region of strong water absorbance around 1645 cm^{-1}, was achieved with the cell path length set to 6—8 μm. To avoid protein denaturation, the gold-grid working electrode was chemically modified by a 2 mM solution of cysteamine reported,[42] but including 1 mM mercaptopropionic acid. To accelerate the redox reaction, a mixture of 15 mediators was used at a final concentration of 45 μM each.[43] At the given concentrations, and with the path length below 10 μm, no spectral contributions from the mediators in the visible and IR range used could be detected in control experiments with samples lacking the protein. Approximately 6–7 μL of the protein solution were sufficient to fill the spectroelectrochemical cell. Potentials were measured against an Ag/AgCl/3 M KCl reference electrode and 208 mV were added to obtain SHE (pH 7) potentials.

FTIR difference spectra as a function of the applied potential were obtained simultaneously from the same sample with a set up combining an IR beam from the interferometer (a modified IFS 25, Bruker, Germany) for the 4000–1000 cm^{-1} range.[40] First, the protein was equilibrated with an initial potential at the electrode, and single-beam spectra in the IR range were recorded. Then a potential step towards the final potential was applied, and single-beam spectra of this state were again recorded after equilibration. Difference spectra were calculated from the two single-beam spectra with the initial single-beam spectrum taken as reference. No smoothing or deconvolution procedures were applied. The equilibration process for each applied potential was followed by monitoring the electrode current and by successively recording spectra in the infrared range until no further changes were observed. The equilibration generally took less than 5 min for the full potential step from −0.3 to 0.7 V. Typically, 128 interferrograms at 4 cm^{-1} resolution were coadded for each single-beam IR spectrum and Fourier-transformed by using triangular apodization. 10–20 difference spectra were averaged.

Acknowledgements

Support from the Volkswagen-Stiftung to W.H. and SFB 472 to P.H. is gratefully acknowledged. We thank Bianca Rosengarten for a preliminary study and Reinhard Brueckner for the advice on synthesis of Bn- and PMB-protected hydroquinonoic acids. We also thank Manfred Keller and Bettina Knapp for the NMR and ESI mass spectral measurements, respectively, and Christa Reichenbach for excellent technical assistance.

[1] a) W. F. DeGrado, C. M. Summa, V. Pavone, F. Nastri, A. Lombardi, *Annu. Rev. Biochem.* **1999**, *68*, 779–819; b) *Chem. Rev.* **2001**, *101*, 3025–3232; special issue: (Ed.: W. F. DeGrado).

[2] a) D. Eisenberg, W. Wilcox, S. M. Eshita, P. M. Pryciak, S. P. Ho, W. F. DeGrado, *Proteins* **1986**, *1*, 16–22; b) S. P. Ho, W. F. DeGrado, *J. Am. Chem. Soc.* **1987**, *109*, 6751–6758.

[3] a) D. E. Robertson, R. S. Farid, C. C. Moser, J. L. Urbauer, S. E. Mulholland, R. Pidikiti, J. D. Lear, A. J. Wand, W. F. DeGrado, P. L. Dutton, *Nature* **1994**, *368*, 425–432; b) S. S. Huang, R. L. Koder, M. Lewis, A. J. Wand, P. L. Dutton, *Proc. Natl. Acad. Sci. USA* **2004**, *101*, 5536–5541; c) B. R. Gibney, S. E. Mulholland, F. Rabanal, P. L. Dutton, *Proc. Natl. Acad. Sci. USA* **1996**, *93*, 15041–15046; d) J. Kaplan, W. F. DeGrado, *Proc. Natl. Acad. Sci. USA* **2004**, *101*, 11566–11570; e) R. E. Sharp, C. C. Moser, F. Rabanal, P. L. Dutton, *Proc. Natl. Acad. Sci. USA* **1998**, *95*, 10465–10470; f) R. E. Sharp, J. R. Diers, F. Rabanal, P. L. Dutton, *J. Am. Chem. Soc.* **1998**, *120*, 7103–7104; g) C. Tommos, J. J. Skalicky, D. L. Pilloud, A. J. Wand, P. L. Dutton, *Biochemistry* **1999**, *38*, 9495–9507.

[4] a) M. Mutter, S. Vuilleumier, *Angew. Chem.* **1989**, *101*, 551–571; *Angew. Chem. Int. Ed. Engl.* **1989**, *28*, 535–554; b) M. Mutter, G. Tuchscherer, C. Miller, K.-H. Altmann, R. I. Carey, D. F. Wyss, A. M. Labhardt, J. E. Rivier, *J. Am. Chem. Soc.* **1992**, *114*, 1463–1470.

[5] B. L. Nilsson, M. B. Soellner, R. T. Raines, *Annu. Rev. Biophys. Biomol. Struct.* **2005**, *34*, 91–118.

[6] a) H. K. Rau, W. Haehnel, *J. Am. Chem. Soc.* **1998**, *120*, 468–476; b) H. K. Rau, N. DeJonge, W. Haehnel, *Proc. Natl. Acad. Sci. USA* **1998**, *95*, 11526–11531; c) M. Fahnenschmidt, H. K. Rau, R. Bittl, W. Haehnel, W. Lubitz, *Chem. Eur. J.* **1999**, *5*, 2327–2334; d) M. Fahnenschmidt, R. Bittl, H. K. Rau, W. Haehnel, W. Lubitz, *Phys. Chem. Chem. Phys.* **2001**, *3*, 4082–4090; e) T. Albrecht, W. W. Li, J. Ulstrup, W. Haehnel, P. Hildebrandt, *PhysChemPhys* **2005**, *6*, 961–968.

[7] a) H. K. Rau, N. DeJonge, W. Haehnel, *Angew. Chem.* **2000**, *112*, 256–259; *Angew. Chem. Int. Ed.* **2000**, *39*, 250–253; b) R. Schnepf, P. Hörth, E. Bill, K. Wieghardt, P. Hildebrandt, W. Haehnel, *J. Am. Chem. Soc.* **2001**, *123*, 2186–2195; c) R. Schnepf, W. Haehnel, K. Wieghardt, P. Hildebrandt, *J. Am. Chem. Soc.* **2004**, *126*, 14389–14399; d) W. Haehnel, *Mol. Diversity* **2004**, *8*, 219–229.

[8] a) R. A. Morton, *Biochemistry of Quinones* **1965**, Academic Press, London; b) *Function of Quinones in Energy Conserving Systems* (Ed.: B. L. Trumpower), Academic press, London, **1982**; c) *Methods in Enzymology, Vol. 378 and 382* (Eds.: H. Sies, L. Packer), Elsevier Academic Press, London, **2004**.

[9] C. Anthony, *Arch. Biochem. Biophys.* **2004**, *428*, 2–9.

[10] a) V. L. Davidson, *Adv. Protein Chem.* **2001**, *59*, 95–140; b) J. E. Dove, J. P. Klinmann, *Adv. Protein Chem.* **2001**, *59*, 141–174.

[11] a) I. Vandenberghe, J. Kim, B. Devreese, A. Hacisalihoglul, H. Iwabuki, T. Okajima, S. Kuroda, O. Adachi, J. A. Jongejani, J. A. Duinel, K. Tanizawa, J. V. Beeumen, *J. Biol. Chem.* **2001**, *276*, 42923–42931; b) S. Datta, Y. Mori, K. Takagi, K. Kawaguchi, Z. Chen, T. Okajima, S. Kuroda, T. Ikeda, K. Kano, K. Tanizawa, F. S. Mathews, *Proc. Natl. Acad. Sci. USA* **2001**, *98*, 14268–14273.

[12] a) M. De Rosa, S. De Rosa, A. Gambacorta, L. Minale, R. H. Thomson, R. D. Worthington, *J. Chem. Soc. Perkin Trans. 1* **1977**, *6*, 653–657; b) G. Schaefer, S. Anemueller, *Eur. J. Biochem.* **1990**, *191*, 297–305; c) T. M. Bandeiras, C. A. Salgueiro, H. Huber, C. M. Gomes, M. Teixeira, *Biochim. Biophys. Acta* **2003**, *1557*, 13–19.

[13] M. Ishii, T. Kawasumi, Y. Igarashi, T. Kodama, Y. Minoda, *J. Bacteriol.* **1987**, *169*, 2380–2384.

[14] P. D. Barker, S. J. Ferguson, *Structure* **1999**, *7*, R281–R290.

[15] a) M. Mewies, W. S. McIntire, N. S. Scrutton, *Protein Sci.* **1998**, *7*, 7–20; b) A. Hassan-Abdallah, R. C. Bruckner, G. Zhao, M. S. Jorns, *Biochemistry* **2005**, *44*, 6452–6462; c) H. Sato, T. Iwata, S. Tokutomi, H. Kandori, *J. Am. Chem. Soc.* **2005**, *127*, 1088–1089.

[16] a) C. D. Fairchild, A. N. Glazer, *J. Biol. Chem.* **1994**, *269*, 28988–28996; b) T. Lamparte, N. Michael, O. Caspani, T. Miyata, K. Shirai, K. Inomata, *J. Biol. Chem.* **2003**, *278*, 33786–33792.

[17] a) J. Deisenhofer, H. Michel, *EMBO J.* **1989**, *8*, 2149–2170; b) S. Iwata, J. Barber, *Curr. Opin. Struct. Biol.* **2004**, *14*, 447–453.

[18] a) W. W. Li, M. Sommerhalter, W. Lubitz, T. Carell, W. Haehnel in *Peptides 2002, Proceedings of the 27th European Peptide Symposium* (Eds.: E. Benedetti, C. Pedone), Edition Ziino, Napoli, Italy, **2002**, pp. 192–193; b) W. W. Li, M. Ritter, P. Hellwig, W. Haehnel in *Peptides Evolution: Genomics, Proteomics & Therapeutics, Proceedings of the 18th American Peptide Symposium* (Eds.: M. Chorev, T. Sawyr), Boston, MA, USA, **2003**, pp. 303–304; c) S. Hay, B. B. Wallace, T. A. Smith, K. P. Ghiggino, T. Wydrzynski, *Proc. Natl. Acad. Sci. USA* **2004**, *101*, 17675–17680; d) W. W. Li, J. Heinze, W. Haehnel, *J. Am. Chem. Soc.* **2005**, *127*, 6140–6141.

[19] a) W. Maentele, *Trends Biochem. Sci.* **1993**, *18*, 197–202; b) J. Breton, E. Nabedryk, *Biochim. Biophys. Acta* **1996**, *275*, 84–90.

[20] a) C. Berthomieu, E. Nabedryk, W. Mäntele, J. Breton, *FEBS Lett.* **1990**, *269*, 363–367; b) S. Buchanan, H. Michel, K. Gerwert, *Biochemistry* **1992**, *31*, 1314–1322; c) F. Baymann, D. E. Robertson, P. L. Dutton, W. Mäntele, *Biochemistry* **1999**, *38*, 13188–13199; d) P. Hellwig, T. Mogi, F. L. Tomson, R. B. Gennis, J. Iwata, H. Miyoshi, W. Mäntele, *Biochemistry* **1999**, *38*, 14683–14689; e) J. Zhang, W. Oettmeier, R. B. Gennis, P. Hellwig, *Biochemistry* **2002**, *41*, 4612–4617; f) P. Hellwig, C. M. Gomes, M. Teixeira, *Biochemistry* **2003**, *42*, 6179–6184.
[21] F. Albericio, I. Annis, M. Royo, G. Barany in *Fmoc Solid Phase Peptide Synthesis, A Practical Approach* (Eds.: W. C. Chan, P. D. White), Oxford University Press, **2000**, pp. 77–114.
[22] T. J. Monks, R. J. Highet, S. S. Lau, *Mol. Pharmacol.* **1990**, *38*, 121–127.
[23] T. W. Greene, P. G. M. Wuts, *Protective Groups in Organic Synthesis*, 2nd ed., Wiley, **1999**, pp. 267–271.
[24] S. A. Kates, N. A. Solé, C. R. Johnson, D. Hudson, G. Barany, F. Albericio, *Tetrahedron Lett.* **1993**, *34*, 1549–1552.
[25] R. H. Thomson, *J. Chem. Soc.* **1953**, 1196–1199.
[26] H. W. Moore, *Science* **1977**, *197*, 527–532.
[27] R. Adams, T. A. Geissman, B. R. Baker, H. M. Teeter, *J. Am. Chem. Soc.* **1941**, *63*, 528–534.
[28] S. Itoh, M. Ogino, S. Haranou, T. Terasaka, T. Ando, M. Komatsu, Y. Ohshiro, S. Fukuzumi, K. Kano, K. Takagi, T. Ikeda, *J. Am. Chem. Soc.* **1995**, *117*, 1485–1493.
[29] D. S. Tarbell, D. K. Fukushima, *J. Am. Chem. Soc.* **1946**, *68*, 1456–1460.
[30] D. O. Mack, M. Wolfensberger, J. M. Girardot, J. A. Miller, B. C. Johnson, *J. Biol. Chem.* **1979**, *254*, 2656–2664.
[31] Y. H. Chen, J. T. Yang, K. H. Chau, *Biochemistry* **1974**, *13*, 3350–3359.
[32] S. Y. M. Lau, A. K. Tanejia, R. S. Hodges, *J. Biol. Chem.* **1984**, *259*, 13253–13261.
[33] a) R. C. Lawson, A. Ferrer, W. Flores, A. E. Alegria, *Chem. Res. Toxicol.* **1999**, *12*, 850–854; b) A. Kröger, S. Biel, J. Simon, R. Gross, G. Unden, C. R. D. Lancaster, *Biochim. Biophys. Acta* **2002**, *1553*, 23–38.
[34] St. Berger, A. Rieker in *The Chemistry of Quinonoid Compounds* (Eds.: S. Patai, Z. Rappoport), Wiley, New York, **1974**, Section I, Chapter 4.
[35] G. D. Buffinton, K. Öllinger, A. Brunmark, E. Cadenas, *Biochem. J.* **1989**, *257*, 561–571.
[36] J. Mauzeroll, A. J. Bard, *Proc. Natl. Acad. Sci. USA* **2004**, *101*, 7862–7867.
[37] A. Brunmark, E. Cadenas, *Free Radical Biol. Med.* **1989**, *7*, 435–477.
[38] a) E. Takahashi, T. A. Wells, C. A. Wraight, *Biochemistry* **2001**, *40*, 1020–1028; b) L. Rinyu, E. W. Martin, E. Takahashi, P. Maróti, C. A. Wraight, *Biochim. Biophys. Acta* **2004**, *1655*, 93–101.
[39] a) J. Breton, C. Boullais, J. R. Burie, E. Nabedryk, C. Mioskowski, *Biochemistry* **1994**, *33*, 14378–14386; b) J. Breton, J. R. Burie, C. Berthomieu, G. Berger, E. Nabedryk, *Biochemistry* **1994**, *33*, 4953–4965.
[40] a) W. W. Li, T. Carell, W. Haehnel in *Peptides Evolution: Proteomics, Genomic & Therapeutics, Proceedings of the 18th American Peptide Symposium* (Eds.: M. Chorev, T. Sawyr), Boston, MA, USA, **2003**, pp. 265–266; b) W. W. Li, W. Haehnel in *Peptides 2004, Proceedings of the 3rd International and 28th European Peptide Symposium* (Eds.: M. Flegel, M. Fridkin, C. Gilon, J. Slaninova), Prague, Czech Republic, Kenes International, **2005**, pp. 46–47.
[41] P. Hellwig, J. Behr, C. Ostermeier, O.-M. H. Richter, U. Pfitzner, A. Odenwald, B. Ludwig, H. Michel, W. Mäntele, *Biochemistry* **1998**, *37*, 7390–7399.
[42] D. A. Moss, E. Nabedryk, J. Breton, W. Mäntele, *Eur. J. Biochem.* **1990**, *187*, 565–572.
[43] P. Hellwig, D. Scheide, S. Bungert, W. Mäntele, T. Friedrich, *Biochemistry* **2000**, *39*, 10884–10891.

Received: October 4, 2005
Revised: March 3, 2006
Published online: July 3, 2006

